Boundary Effects on the Sedimentation and Hindered Diffusion of Charged Particles

Narahari S. Pujar and Andrew L. Zydney
Dept. of Chemical Engineering, University of Delaware, Newark, DE 19716

A general formalism is developed to examine the sedimentation of a charged particle in a bounded system at small Peclet numbers and small particle-surface potentials. The excess viscous force is evaluated using a generalized form of the Lorentz reciprocal theorem, eliminating the need to calculate the detailed fluid flow around the charged particle. Specific calculations are provided for the sedimentation of a charged sphere in a concentric (uncharged) spherical cavity. Boundary interactions increase the magnitude of the excess force at small Debye lengths, with the opposite effect seen at very large Debye lengths. A general solution is presented for the sedimentation velocity for an arbitrary particle in both unbounded and bounded systems in the limit of very thin double layers. The excess force under these conditions is proportional to the square of the Debye length, with the proportionality constant being a function of the detailed system geometry. These results provide important insights into the transport of charged particles in porous membranes and chromatographic materials.

Introduction

The hindered sedimentation and diffusion of uncharged particles has been studied quite extensively in a variety of geometries, with much of this work described in a review article by Deen (1987). The presence of the boundary increases the hydrodynamic drag on the particle, significantly reducing the sedimentation velocity from that which would be found in an infinite medium under identical conditions. The hindered (or effective) particle diffusion coefficient in membranes and other porous media can be evaluated from the force on the sedimenting particle using Einstein's approach, with the results found to be in good agreement with available experimental data (Deen, 1987).

There is considerable experimental evidence that the rate of colloidal transport in bounded systems is significantly altered by electrical interactions between the colloid and the boundary. For example, Pujar and Zydney (1994) found more than a two order of magnitude reduction in the rate of protein transport through narrow pore membranes due to changes in electrolyte shielding (i.e., salt concentration). Likewise, Potschka (1988) found that the pH and ionic strength of the eluent significantly affected the retention of various polyelectrolytes during both size-exclusion and ion-exchange chromatography. This behavior has generally been attributed to electrostatic exclusion (i.e., thermodynamic partitioning) effects, at least in part because there are currently no analyses to describe the role of the electrostatic interactions on hindered diffusive transport through these porous media.

The motion of a charged particle is considerably more complex than that of an uncharged particle due to the deformation of the electrical double layer arising from the fluid flow around the particle (the relaxation effect). The fluid flow tends to drag the counterions (i.e., the positive ions surrounding a negatively charged particle) up and around the particle, resulting in an excess in the concentration of coions in the region immediately beneath the particle. This distortion of the electrical double layer gives rise to an induced (vertical) electric field. This sedimentation potential was first discovered by Dorn in 1878 and is often referred to as the Dorn effect. This induced potential not only exerts a body force on the particle, it also alters the velocity and pressure profiles in the fluid due to its action on the electrolyte. This velocity disturbance reduces the hydrodynamic drag on the particle compared to that on an uncharged particle.

The first theoretical analysis of these effects was presented by Smoluchowski (1921) for a sphere with an infinitely thin double layer. The sedimentation velocity for a charged sphere was shown to be smaller than that for an uncharged sphere

Correspondence concerning this article should be addressed to A. L. Zydney.

by a term that is proportional to the square of the particle surface potential. Booth (1954) evaluated the sedimentation potential and the sedimentation velocity for an isolated sphere with arbitrary double layer thickness using a perturbation expansion in the particle surface potential, with complex expressions for the necessary coefficients presented for the first-order corrections. The maximum correction to the sedimentation velocity occurs when the double layer thickness is approximately equal to the particle radius. Oshima et al. (1984) subsequently generalized these derivations and presented numerical results for the sedimentation velocity at both small and large surface potential.

Corresponding analyses for the hindered sedimentation of a charged sphere in bounded geometries are currently unavailable. Bike and Prieve (1990) and van de Ven et al. (1993) examined the normal force (or electrokinetic lift) on a charged sphere sliding past a flat plate, and Keh and Anderson (1985) and Zydney (1995) examined the effects of boundary interactions on the electrophoretic mobility of a charged sphere in different pore geometries. Thies-Weesie et al. (1995) modeled the effect of salt concentration on the sedimentation velocity at different particle volume fractions by accounting for changes in the hydrodynamic interaction caused by the structure of the suspension. None of these analyses can be directly extended to the sedimentation of a charged particle in a bounded system because of the complex coupling between the fluid flow, the ion concentrations, and the potential field in this problem, in addition to the inherent nonlinearity in the governing equations describing particle sedimentation.

This article describes a general approach for evaluating the sedimentation velocity (and thus the drag force) of an arbitrary nonrotating charged particle in a bounded system for small particle Peclet numbers and small particle-surface potentials. The additional (excess) force arising from the electrical interactions has two components: an electrical force that is directly associated with the induced potential field, and a viscous force that arises from the alteration in the velocity profiles associated with the interaction between the electric field and the electrolyte. This latter force is evaluated using a generalized form of the Lorentz reciprocal theorem (Happel and Brenner, 1973; Kim and Karrila, 1991) developed by Tuebner (1982), thereby eliminating the need to actually determine the complex velocity and pressure profiles describing the motion of the charged sphere. Specific calculations are provided for the sedimentation of a charged sphere in both an infinite medium and a spherical cavity. The symmetry in the latter geometry reduces the partial differential equations describing the hydrodynamic and electrical interactions to simple ordinary differential equations. A general solution for the sedimentation velocity of an arbitrary particle in both an unbounded and bounded system is developed in the limit of very thin double layers using the method of Green's functions. The dimensionless excess force under these conditions is shown to be proportional to $(\kappa a)^{-2}$ irrespective of the detailed system geometry. The final section of the manuscript examines the implications of these results for the hindered transport of charged colloids (e.g., proteins) through porous membranes and chromatographic materials.

Theoretical Development

The governing equations describing the sedimentation of an arbitrary particle in a bounded system are given by the Navier–Stokes equations:

$$\mu\nabla^2 \boldsymbol{v}^* = \nabla P^* - \rho \boldsymbol{g}^* + \rho_E \nabla\Phi^* \tag{1}$$

$$\nabla\cdot\mathbf{v}^* = 0 \tag{2}$$

where $\boldsymbol{v}^*$ is the fluid velocity, P^* is the hydrostatic pressure, $\boldsymbol{g}^*$ is the gravitational body force, and ρ and μ are the fluid density and viscosity, respectively. The local electrical potential (Φ^*) and the local charge density (ρ_E) are related by Poisson's equation:

$$\nabla^2\Phi^* = -\frac{\rho_E}{\epsilon} = -\frac{F}{\epsilon}\Sigma z_i C_i^*, \tag{3}$$

where C_i^* is the ion concentration, z_i is the ion valence, ϵ is the dielectric constant of the electrolyte solution, and F is Faraday's constant. The conservation equation for the ions is

$$\frac{\partial C_i^*}{\partial t} = -\nabla\cdot N_i^*. \tag{4}$$

The ion flux (N_i^*) has contributions from convection, diffusion, and electrical conduction:

$$N_i^* = \boldsymbol{v}C_i^* - D_i\left[\nabla C_i^* + \frac{z_i F}{RT} C_i^* \nabla\Phi^*\right], \tag{5}$$

where D_i is the ion diffusivity, R is the ideal gas constant, and T is the absolute temperature.

Equations 1–5 are nondimensionalized using the characteristic velocity (D_+/a), the characteristic particle dimension (a), the ion concentration at zero electrical potential (C_∞), and the particle surface potential (Φ_a) yielding:

$$\nabla^2\boldsymbol{v} = \nabla P - \rho\boldsymbol{g} + \beta\zeta_a^2\nabla\Psi\nabla^2\Psi \tag{6}$$

$$\nabla\cdot\boldsymbol{v} = 0 \tag{7}$$

$$\zeta_a\nabla^2\Psi = -\frac{1}{2}(\kappa a)^2(C_+ - C_-) \tag{8}$$

$$\boldsymbol{v}\cdot\nabla C_+ = \nabla[\nabla C_+ + \zeta_a C_+\nabla\Psi] \tag{9}$$

$$\boldsymbol{v}\cdot\nabla C_- = q\nabla[\nabla C_- - \zeta_a C_-\nabla\Psi], \tag{10}$$

where we have assumed that the ion concentrations are at quasi-steady state and we have limited our analysis to a symmetric (1:1) electrolyte. Equations 6 to 10 are expressed in terms of four dimensionless parameters: the dimensionless surface potential,

$$\zeta_a = \frac{F\Phi_a}{RT}, \tag{11}$$

the dimensionless inverse double layer thickness,

$$\kappa a = \left(\frac{2F^2a^2C_\infty}{\epsilon RT}\right)^{1/2}, \tag{12}$$

(where κ^{-1} is the Debye length), the ratio of the ion diffusivities,

$$q = \frac{D_-}{D_+}, \tag{13}$$

and a dimensionless electrical force constant

$$\beta = \frac{\epsilon}{\mu D_+}\left(\frac{RT}{F}\right)^2. \tag{14}$$

The difficulty in solving Equations 6–10 lies in the nonlinearity of both the Navier–Stokes equation and the ion conservation equations in addition to the coupling between the fluid flow, the ion concentration profiles, and the electrical potential. Following van de Ven (1989), we look to develop a solution for small Peclet numbers:

$$Pe = \frac{Ua}{D_+}, \tag{15}$$

where U is the sedimentation velocity. Under these conditions the electrical double layer is only slightly perturbed from equilibrium. Thus we can express the required variables using the first two terms in a perturbation expansion in Pe:

$$\boldsymbol{v} = Pe\,\boldsymbol{v}_1 \tag{16a}$$

$$C_i = C_{i0} + PeC_{i1} \tag{16b}$$

$$\Psi = \Psi_0 + Pe\Psi_1 \tag{16c}$$

$$P = P_0 + PeP_1. \tag{16d}$$

Note that the zeroth-order term for the velocity is absent since the solution at $Pe = 0$ corresponds to the equilibrium (nonsedimenting) problem.

Equilibrium (zeroth-order) solution

The governing equations to zeroth order in Pe are

$$\nabla P_0 + \beta\zeta_a^2\nabla\Psi_0\nabla^2\Psi_0 - \rho\boldsymbol{g} = 0 \tag{17}$$

$$\zeta_a\nabla^2\Psi_0 = -\frac{1}{2}(\kappa a)^2(C_{+0} - C_{-0}) \tag{18}$$

$$\nabla\cdot[\nabla C_{i0} + z_i\zeta_a C_{i0}\nabla\Psi_0] = 0. \tag{19}$$

Equation 19 can be immediately integrated to give the Boltzmann distribution:

$$C_{i0} = \exp[-z_i\zeta_a\Psi_0] \tag{20}$$

so that Eq. 18 becomes

$$\zeta_a\nabla^2\Psi_0 = (\kappa a)^2\sinh(\zeta_a\Psi_0). \tag{21}$$

Analytical solutions for the equilibrium potential (Ψ_0) are available only for certain well-defined geometries and under very limited conditions (e.g., large κa or small ζ_a). Equation 21 can, at least in principle, be solved numerically for more complex geometries and arbitrary double layer thickness and surface potential. Once the equilibrium potential is known, the pressure field can be evaluated directly from Eq. 17. The zeroth-order contribution to the force is then determined from P_0 and Ψ_0. Note that the equilibrium electrical potential term provides no contribution to the net force (in the direction of the gravitational field) for a system that is symmetric about the equatorial plane of the particle (oriented perpendicular to the direction of the gravitational field).

First-order (perturbation) solution

The governing equations to first order in Pe are

$$\nabla^2\boldsymbol{v}_1 = \nabla P_1 + \beta\zeta_a^2[\nabla\Psi_0\nabla^2\Psi_1 + \nabla\Psi_1\nabla^2\Psi_0] \tag{22}$$

$$\nabla\cdot\boldsymbol{v}_1 = 0 \tag{23}$$

$$\zeta_a\nabla^2\Psi_1 = -\frac{1}{2}(\kappa a)^2(C_{+1} - C_{-1}) \tag{24}$$

$$\boldsymbol{v}_1\cdot\nabla C_{+0} = \nabla\cdot[\nabla C_{+1} + \zeta_a C_{+1}\nabla\Psi_0 + \zeta_a C_{+0}\nabla\Psi_1] \tag{25}$$

$$\boldsymbol{v}_1\cdot\nabla C_{-0} = q\nabla\cdot[\nabla C_{-1} - \zeta_a C_{-1}\nabla\Psi_0 - \zeta_a C_{-0}\nabla\Psi_1]. \tag{26}$$

We seek a solution to Eqs. 22–26 that is valid for small values of the particle-surface potential. Following van de Ven (1989), we express the velocity, pressure, and ion concentrations as

$$\boldsymbol{v}_1 = \boldsymbol{u}_0 + \zeta_a^2\boldsymbol{u}_1 \tag{27a}$$

$$P_1 = p_0 + \zeta_a^2 p_1 \tag{27b}$$

$$C_{i1} = \zeta_a c_{i1}, \tag{27c}$$

where the first-order corrections to the velocity and pressure are of order ζ_a^2, as can be seen from the general form of Eq. 22. Collecting terms up to ζ_a^2 gives

$$\nabla^2\boldsymbol{u}_0 = \nabla p_0 \qquad \nabla\cdot\boldsymbol{u}_0 = 0 \tag{28}$$

$$\nabla^2\boldsymbol{u}_1 = \nabla p_1 + \beta[\nabla\Psi_0\nabla^2\Psi_1 + \nabla\Psi_1\nabla^2\Psi_0] \qquad \nabla\cdot\boldsymbol{u}_1 = 0 \tag{29}$$

$$\nabla^2\Psi_1 = -\frac{1}{2}(\kappa a)^2(c_{+1} - c_{-1}) \tag{30}$$

$$-\boldsymbol{u}_0\cdot\nabla\Psi_0 = \nabla\cdot[\nabla c_{+1} + \nabla\Psi_1] \tag{31}$$

$$\boldsymbol{u}_0\cdot\nabla\Psi_0 = q\nabla\cdot[\nabla c_{-1} - \nabla\Psi_1], \tag{32}$$

where the terms involving C_{i0} have been evaluated using Eq. 20, keeping all terms up to order ζ_a^2. The solution to Eq. 28 is available for spherical particles in a number of different bounded geometries. Equations 30–32 completely define the perturbation potential (Ψ_1) and the corrections to the ion concentrations (c_{+1} and c_{-1}). The real difficulty in evaluating the sedimentation velocity lies in the solution to Eq. 29 due to the complex form of the two potentials (Ψ_0 and Ψ_1). However, as will be shown below, it is actually possible to evaluate the force on the particle, and thus the sedimentation velocity, without explicitly solving for either $\boldsymbol{u}_1$ or p_1 by using a generalized form of the Lorentz reciprocal theorem.

Evaluation of the force

In previous analyses of the sedimentation velocity, the force on the particle has been evaluated by directly integrating the electrical and hydrodynamic stress tensors over the surface of the particle. This requires detailed expressions for the velocity, pressure, and potential fields up to order ζ_a^2. We shall proceed in a very different fashion, following the general approach developed by Tuebner (1982). The total force on the charged particle is expressed as

$$\boldsymbol{F}^*_{\text{total}} = \boldsymbol{F}^*_{\text{uncharged}} + \boldsymbol{F}^*_{\text{electric}} + \boldsymbol{F}^*_{\text{viscous}}, \tag{33}$$

which accounts for (1) the viscous force exerted on the particle in the absence of its charge as well as the force due to gravity ($\boldsymbol{F}^*_{\text{uncharged}}$); (2) the electrical force ($\boldsymbol{F}^*_{\text{electric}}$) exerted on the particle by the induced potential field; and (3) the excess viscous force ($\boldsymbol{F}^*_{\text{viscous}}$) arising from the perturbations in the velocity and pressure fields (given by $\boldsymbol{u}_1$ and p_1) caused by the interaction between the electric field and the electrolyte.

The electric force is evaluated by integrating the electrical stress tensor (σ_E) over the particle surface (Tuebner, 1982):

$$\boldsymbol{F}^*_{\text{electric}} = \int_{S^*_{\text{particle}}} \sigma_E \cdot d\boldsymbol{S}^*, \tag{34}$$

where

$$\sigma_E = \frac{\epsilon}{4\pi}\left[\boldsymbol{EE} - \frac{1}{2}E^2\boldsymbol{I}\right], \tag{35}$$

with $\boldsymbol{E} = -\nabla\Phi^*$ and $\boldsymbol{I}$ the identity matrix. Equation 34 can be simplified by following the approach outlined by Levine et al. (1978), yielding

$$\boldsymbol{F}_{\text{electric}} = \frac{\boldsymbol{F}^*_{\text{electric}}}{6\pi\mu U a} = \frac{\beta}{2}\left(1+\frac{1}{q}\right)\frac{\zeta_a^2}{12} f_e, \tag{36}$$

where

$$f_e = \frac{2}{\pi}\int_{S_{\text{particle}}} (\nabla\Psi_0\cdot\boldsymbol{n})(\nabla\Psi_1\cdot\boldsymbol{k}) + (\nabla\Psi_1\cdot\boldsymbol{n})(\nabla\Psi_0\cdot\boldsymbol{k})\, dS, \tag{37}$$

where $\boldsymbol{k}$ is the unit vector pointing in the same direction as the gravitational, field and $\boldsymbol{n}$ is the unit normal. The electric force, therefore, has two distinct contributions: one arising from the interaction between the induced perturbation potential ($\nabla\Psi_1\cdot\boldsymbol{k}$) and the equilibrium charge on the sphere (which is proportional to $\nabla\Psi_0\cdot\boldsymbol{n}$) and one associated with the interaction between the equilibrium field ($\nabla\Psi_0\cdot\boldsymbol{k}$) and the induced surface charge (which is proportional to $\nabla\Psi_1\cdot\boldsymbol{n}$). The perturbation potential Ψ_1 can be evaluated from Eqs. 30–32 as discussed later.

The viscous force is evaluated using a generalized form of the Lorentz reciprocal theorem, which was developed by Tuebner (1982):

$$\boldsymbol{F}^*_{\text{viscous}} = \int_{V^*} \bar{\rho}_E \boldsymbol{w}\cdot\nabla\Phi^*\, dV^*, \tag{38}$$

where $\boldsymbol{w}$ is the solution to the Navier–Stokes equation for the velocity field around an uncharged particle in the same bounded system moving at a constant (unit) velocity. The volume integral in Eq. 38 can be rewritten as:

$$\int_{V^*}\rho_E\boldsymbol{w}\cdot\nabla\Phi^*\, dV^* = \epsilon\zeta_a^2\int_{V^*}\nabla^2\Psi_0(\boldsymbol{w}\cdot\nabla\Psi_0)dV^* + \epsilon\zeta_a^2 Pe\int_{V^*}[\nabla^2\Psi_0(\boldsymbol{w}\cdot\nabla\Psi_1)+\nabla^2\Psi_1(\boldsymbol{w}\cdot\nabla\Psi_0)]\,dV^* + \epsilon\zeta_a^2 Pe^2\int_{V^*}\nabla^2\Psi_1(\boldsymbol{w}\cdot\nabla\Psi_1)\,dV^*. \tag{39}$$

The last integral in Eq. 39 can be neglected since it is proportional to Pe^2. The term involving $\nabla^2\Psi_0(\boldsymbol{w}\cdot\nabla\Psi_0)$ is exactly zero using the Gauss divergence theorem for a system with uniform potentials on both surfaces. Equation (39) can be further simplified using the linearized form of Eq. 21 for $\nabla^2\Psi_0$ and using Eq. 30 for $\nabla^2\Psi_1$. The resulting volume integral can be expressed in terms of a surface integral using the Gauss divergence theorem yielding:

$$\boldsymbol{F}^*_{\text{viscous}} = \epsilon\zeta_a^2 Pe(\kappa a)^2\left[\int_S \Psi_0\Psi_1\boldsymbol{w}\cdot\boldsymbol{n}\, dS - \frac{1}{2}\int_V s(\boldsymbol{w}\cdot\nabla\Psi_0)\, dV\right], \tag{40}$$

where $s = 2\Psi_1 + c_{+1} - c_{-1}$. Note that the development leading to Eq. 40 uses $\nabla\cdot\boldsymbol{w} = 0$ from the continuity equation. The surface integral in Eq. 40 is set equal to zero for sedimentation at constant surface potential since $\Psi_1 = 0$ at the particle and pore boundaries under these conditions. The dimensionless excess viscous force can thus be evaluated as

$$\boldsymbol{F}_{\text{viscous}} = \frac{\boldsymbol{F}^*_{\text{viscous}}}{6\pi\mu\text{Ua}} = \frac{\beta}{2}\left(1+\frac{1}{q}\right)\frac{\zeta_a^2}{12} f_v, \tag{41}$$

where

$$f_v = -\frac{(\kappa a)^2}{\pi}\int_V s(\boldsymbol{w}\cdot\nabla\Psi_0)\, dV. \tag{42}$$

The quantity s satisfies the differential equation

$$\nabla^2 s = -\left(1+\frac{1}{q}\right)\boldsymbol{u}_0\cdot\nabla\Psi_0, \tag{43}$$

which is developed directly from Eqs. 31 and 32. The appropriate boundary conditions on s are developed from the constraint that there is no ion flux through the particle or pore surface, that is,

$$\boldsymbol{n}\cdot\nabla s = 0 \qquad \text{at all surfaces.} \tag{44}$$

Equation 44 can be replaced by the condition that $s = 0$ as $r \to \infty$ for a particle in an infinite domain. Equation 44 also

ensures that there is no net current flux in this system across the equatorial plane perpendicular to the direction of sedimentation.

The perturbation potential Ψ_1 satisfies the partial differential equation:

$$\nabla^2\Psi_1 - (\kappa a)^2\Psi_1 = -\frac{1}{2}(\kappa a)^2 s, \tag{45}$$

which is developed from Eqs. 30–32. Since the sedimentation is assumed to occur at constant surface potential, Eq. 45 is solved using the boundary conditions that $\Psi_1 = 0$ on both the pore and particle surface.

The quantities s and Ψ_1 are determined entirely by the motion of the uncharged sphere ($\boldsymbol{u}_0$ and $\boldsymbol{w}$) and the equilibrium potential field (Ψ_0). The net force on the particle can thus be calculated directly from Eq. 33, eliminating the need to evaluate the actual (perturbation) velocity and pressure fields surrounding the charged particle ($\boldsymbol{u}_1$ and p_1). The sedimentation velocity is then calculated from the constraint that $\boldsymbol{F}^*_{\text{total}} = 0$ for a freely sedimenting particle. The use of these equations for the evaluation of the sedimentation velocity are illustrated in the following sections for a charged spherical particle in an infinite medium, for a charged spherical particle in a concentric (uncharged) spherical cavity, and for an arbitrary charged particle in a bounded system at very small values of the double layer thickness.

Results and Discussion

Isolated sphere in an infinite medium

The equilibrium electrical potential for an isolated sphere at low surface potentials is evaluated using Eq. 21 by expressing the hyperbolic sine by the first term in its Taylor series expansion yielding:

$$\Psi_0 = \frac{1}{r}\exp[\kappa a(r-1)], \tag{46}$$

where r is the dimensionless radial position. The electrostatic potential in the unbounded system is spherically symmetric, thus the radial component of the velocity vector

$$u_r = -\left[1 - \frac{3}{2r} + \frac{1}{2r^3}\right]\cos\theta \tag{47}$$

provides the only contribution to the righthand side of the differential equation for s (Eq. 43). The quantity s must be proportional to $\cos\theta$ under these conditions so as to match the known angular dependence of u_r. The solution to Eq. 43 can thus be written explicitly using the method of variation of parameters as

$$s = \left[B_1 r + \frac{B_2}{r^2}\right]\cos\theta - \left(\frac{1+q}{3q}\right) r\int_1^r u_r\Psi_0'\,dz + \left(\frac{1+q}{3q}\right)\frac{1}{r^2}\int_1^r z^3 u_r\Psi_0'\,dz, \tag{48}$$

where z is a dummy variable over which the integration is performed. The integration constants B_1 and B_2 are evaluated from the boundary conditions (Eq. 44) yielding:

$$B_1 = 2B_2 = \frac{1+q}{3q}\int_1^\infty \frac{u_r}{\cos\theta}\Psi_0'\,dz. \tag{49}$$

Substitution of Eqs. 46 and 47 into Eq. 49 yields

$$B_1 = \left(\frac{1+q}{2q}\right)\exp(\kappa a)[E_3(\kappa a) - E_5(\kappa a)], \tag{50}$$

where $E_n(x)$ is the exponential integral defined as

$$E_n(x) = x^{n-1}\int_x^\infty \frac{\exp(-t)}{t^n}\,dt = \int_1^\infty \frac{\exp(-tx)}{t^n}\,dt. \tag{51}$$

For a sphere in an unbounded (infinite) domain, Eq. 37 can be rewritten in terms of a volume integral using the Gauss divergence theorem:

$$f_e = \frac{(\kappa a)^2}{\pi}\int_V s(\boldsymbol{k}\cdot\nabla\Psi_0)\,dV, \tag{52}$$

where the second (boundary) surface has been taken at a distance arbitrarily far from the particle where Ψ_0 and Ψ_1 vanish (i.e., well outside the electrical double layer). In deriving Eq. 52 we have evaluated $\nabla^2\Psi_0$ and $\nabla^2\Psi_1$ using Eqs. 21 and 30, respectively. The electric force can be evaluated analytically under these conditions using the expression for s given by Eqs. 48–50:

$$f_e = 4(\kappa a)^2\left[\frac{1}{12}\exp(\kappa a)[4E_0(\kappa a) - 6E_1(\kappa a) + 5E_3(\kappa a) + 3E_4(\kappa a) - 6E_5(\kappa a)] - \exp(2\kappa a)E_1(2\kappa a)\right]. \tag{53}$$

The viscous force is evaluated in a similar manner from Eq. 42:

$$f_v = \left(\frac{1+q}{2q}\right)\Big[\exp(2\kappa a)[3E_4(\kappa a) - 4E_6(\kappa a)]^2 + 8\exp(\kappa a)[E_3(\kappa a) - E_5(\kappa a)] - \exp(2\kappa a)[4E_3(2\kappa a) + 3E_4(2\kappa a) - 7E_8(2\kappa a)]\Big] - 4\left(\frac{1+q}{2q}\right)(\kappa a)^2\left[\frac{1}{12}\exp(\kappa a)[4E_0(\kappa a) - 6E_1(\kappa a) + 5E_3(\kappa a) + 3E_4(\kappa a) - 6E_5(\kappa a)] - \exp(2\kappa a)E_1(2\kappa a)\right]. \tag{54}$$

The total dimensionless excess force ($f = f_e + f_v$) is thus

$$f = \left(\frac{1+q}{2q}\right)\Big[\exp(2\kappa a)[3E_4(\kappa a) - 4E_6(\kappa a)]^2 + 8\exp(\kappa a)[E_3(\kappa a) - E_5(\kappa a)] - \exp(2\kappa a)[4E_3(2\kappa a) + 3E_4(2\kappa a) - 7E_8(2\kappa a)]\Big]. \quad (55)$$

Equation 55 can also be developed from a single volume integral given by the sum of Eqs. 42 and 52:

$$f = -\frac{(\kappa a)^2}{\pi}\int_V s(\boldsymbol{u}_0\cdot\nabla\Psi_0)\,dV, \quad (56)$$

which avoids the need to evaluate both f_v and f_e separately. Equation 55 was derived previously using a much more complicated analysis involving direct integration of the hydrodynamic and electrical stresses by Booth (1954) and later by Oshima (1984). The dependence of f on κa is examined in more detail toward the end of the next section.

Spherical particle in a spherical cavity

In order to investigate the effects of boundary interactions on the sedimentation of a charged particle, we have examined the motion of a single charged sphere sedimenting at the center of a spherical cavity. The spherical symmetry in this system greatly simplifies the solution of the governing equations while providing important insights into the magnitude of the boundary effects and their dependence on both the particle/pore size and κa. This type of spherical geometry has been used previously in the analysis of boundary interactions on solute partitioning (Giddings et al. 1968; Glandt, 1980, 1981), hydrodynamic drag (Haberman and Sayre, 1958), and hindered electrophoretic motion (Zydney, 1995).

The equilibrium electrostatic potential in this system is given as

$$\Psi_0 = \frac{1}{r}\left[\frac{\sinh\left[\kappa a\left(\frac{1}{\lambda}-r\right)\right]}{\sinh\left[\kappa a\left(\frac{1}{\lambda}-1\right)\right]} + \frac{\alpha}{\lambda}\frac{\sinh[\kappa a(r-1)]}{\sinh\left[\kappa a\left(\frac{1}{\lambda}-1\right)\right]}\right], \quad (57)$$

where we have used constant surface potential boundary conditions on both the particle and pore surfaces. Equation 57 is expressed in terms of two new dimensionless parameters: that is, $\lambda = a/b$ is the ratio of particle to pore radii, and $\alpha = \zeta_b/\zeta_a$ is the ratio of pore to particle surface potentials. The highest order contribution to the velocity is evaluated from Eq. 28, yielding

$$u_r = \left[A_1 r^2 + \frac{A_2}{r} + A_3 + \frac{A_4}{r^3}\right]\cos\theta. \quad (58)$$

The constants A_1–A_4 are given by Haberman and Sayre (1958) as well as by Happel and Brenner (1973) as functions of λ. The quantity s is again proportional to cos θ. The solution to s is given by Eq. 48 but the integration constants are now expressed as

$$B_1 = 2B_2 = \frac{1+q}{6q(1-\lambda^3)}\int_1^{1/\lambda}\frac{(1+2z^3\lambda^3)}{(1-\lambda^3)}\left[\frac{u_r}{\cos\theta}\right]\Psi_0'\,dz. \quad (59)$$

The integrals in Eqs. 48 and 59 were evaluated numerically for specified values of κa and λ using the IMSL routine DQDAG, which employs a globally adaptive integration scheme based on the Gauss–Kronrod method. The perturbation potential in this system is also proportional to cos θ, with the radial dependence of Ψ_1 evaluated numerically from Eq. 45 employing the same numerical technique. Finally, the viscous force was evaluated by numerical integration of Eq. 42 using the IMSL routine DQDAGS. Analytical expressions for s, f_e, and f_v were also developed at both small and large κa.

The calculated values of the dimensionless viscous (f_v) and electrical (f_e) forces for a charged spherical particle in a spherical cavity (with $\zeta_b = 0$) are shown in Figure 1 as a function of κa for several values of λ. All calculations were performed with $q = 1$ for simplicity. Note that the electrical force has been plotted as negative f_e, that is, the viscous and electrical forces act in opposite directions under all conditions. The electrical force opposes the particle sedimentation, while the alteration in the velocity profiles actually reduces the drag on the charged sphere. This latter effect can be thought of in terms of an apparent slip velocity at the particle surface associated with the perturbation velocity, $\boldsymbol{u}_1$. Both the dimensionless viscous and electrical forces become independent of κa as $\kappa a \to \infty$. The equilibrium potential (Ψ_0) at large κa becomes independent of λ, while the potential gradient at the particle surface (i.e., the particle-surface charge density) becomes proportional to κa. Both s and Ψ_1 are proportional to $(\kappa a)^{-2}$ under these conditions, although the gradient of Ψ_1 is proportional to $(\kappa a)^{-1}$. The net result is that both f_v and f_e become independent of κa with equal magnitudes (to highest order in κa):

$$f_v = -f_e = \left[\frac{(2-\lambda^3+3\lambda^5)(1-2\lambda^3)}{2(1-\lambda^3)(4-9\lambda+10\lambda^3-\lambda^5+4\lambda^6)}\right]. \quad (60)$$

In this large κa limit, all three contributions to the current flow (convective, diffusive, and conductive)

$$N_+ - N_- = -Pe\zeta_a\left[2\nabla\Psi_1 + \nabla(c_{+1}-c_{-1}) + \left(1+\frac{1}{q}\right)\boldsymbol{u}_0\Psi_0\right] \quad (61)$$

are proportional to $(\kappa a)^{-2}$. The sharp increase in $-f_e$ and f_v with increasing λ arises from the corresponding increase in the velocity gradient near the surface of the particle. Both f_v and f_e are directly proportional to the second derivative of u_r with respect to r (evaluated at the particle surface) under these conditions. This behavior is discussed in more detail subsequently.

The dimensionless viscous and electric forces become proportional to $(\kappa a)^2$ at small κa for $\lambda = 0.2$, 0.4, 0.6, and 0.8. For $\kappa a < \lambda$, the electrical double layer spans the entire spherical cavity, thus the equilibrium potential becomes inde-

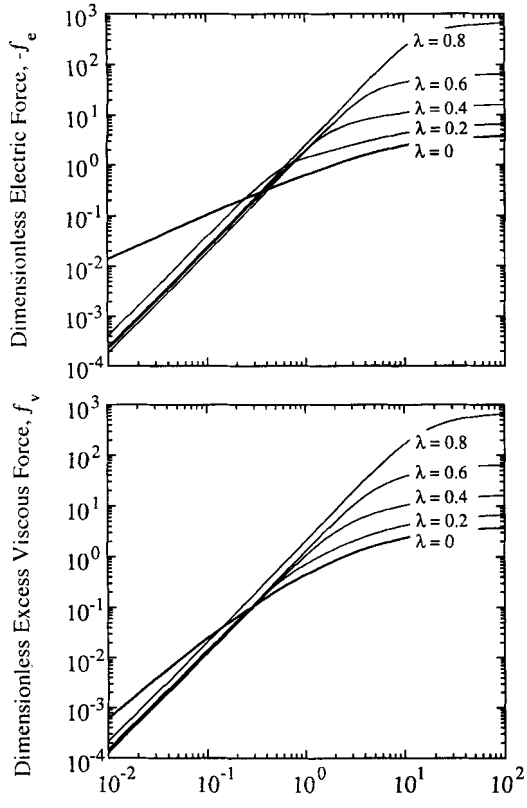

Figure 1. Dimensionless electric (top panel) and excess viscous (bottom panel) forces as a function of κa.

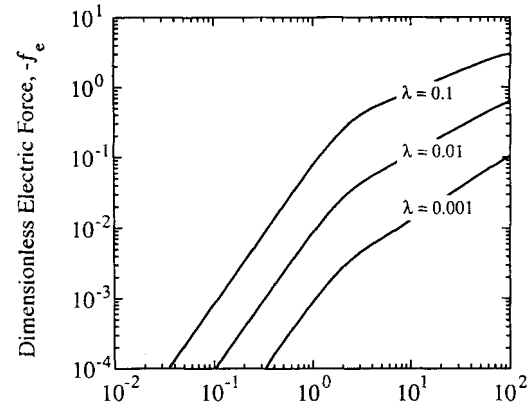

Figure 2. Dimensionless electric force as a function of κb at small λ.

pendent of κa. The quantity s (determined from Eq. 48) is also independent of κa under these conditions. The first nonzero contribution to the perturbation potential (Ψ_1) for $\kappa a < \lambda$ is also proportional to $(\kappa a)^2$. This ensures that the convective current flow (which is proportional to $C_{+0} - C_{-0}$ and thus Ψ_0) is exactly balanced by the diffusive current flow (which is proportional to $\nabla(c_{+1} - c_{-1})$) with the electrophoretic current being negligible. The net result is that $-f_e$ (evaluated from Eq. 37) and f_v (from Eq. 42) both become proportional to $(\kappa a)^2$ at small κa. In contrast to the preceding behavior, the electrical force when $\lambda = 0$ is linearly proportional to κa at small κa (Figure 1). The behavior at small κa and at small λ is discussed in more detail subsequently. The transition from the small to large κa behavior occurs when the electrical double layer becomes smaller than the size of the spherical cavity, that is, when κa is of order $\lambda/(1-\lambda)$. This physical picture is in good agreement with the results in Figure 1, which shows more than an order-of-magnitude increase in the transition value of κa as λ goes from 0.2 to 0.8.

The behavior of the electrical force at small κa and small λ is examined in more detail in Figure 2. The results are plotted as a function of $\kappa b = \kappa a/\lambda$ for $\lambda = 0.001$, 0.01, and 0.1. When $\kappa b \ll 1$, the dimensionless electrical force is proportional to $(\kappa b)^2$ [or $(\kappa a)^2$]. When $\kappa b > 1$ and $\kappa a \ll 1$, however, $-f_e$ varies linearly with κa. This linear dependence on κa was seen in Figure 1 for $\lambda = 0$ since κb is infinite in the unbounded problem. The very different behavior in these systems arises from the complex effects of the boundary on the equilibrium and perturbation potentials. The leading term in the equilibrium potential becomes independent of κa at very small κa; however, the next term (in a perturbation expansion in κa) is linear in κa for $\lambda = 0$, but varies as $(\kappa a)^2$ for $\lambda > \kappa a$ (see Eqs. 46 and 57). The κa independent term in Ψ_0 provides no contribution to Ψ_1; the difference in the higher order terms gives rise to the different behavior seen in Figure 1. The magnitude of the perturbation potential is also determined by the details of the velocity profile u_0. In the unbounded problem, u_0 decays from its value at the particle surface (U) to zero as $r \to \infty$. The velocity profile in the bounded problem is quite different, with a recirculation (reverse) flow occurring in the region near the outer boundary in order to satisfy the overall continuity equation. This effect is discussed in more detail by Zydney (1995) in the context of particle electrophoresis. At small κa, this recirculation generates a reverse current flow near the outer boundary, which reduces the magnitude of the perturbation potential required to satisfy the no net current constraint. The combination of these effects leads to the $(\kappa b)^2$ dependence at small κb seen in Figure 2. In contrast the behavior for $\kappa b > 1$ and $\kappa a \ll 1$ resembles that in the unbounded system.

The dependence of the viscous and electrical forces on λ is shown explicitly in Figure 3. Results for λ close to 1 are not shown because of numerical difficulties. At large κa, the velocity gradient at the particle surface increases with increasing λ. This causes an increase in both the perturbation potential and s leading to the observed increase in both $-f_e$ and f_v with increasing λ. The behavior at small κa (e.g., $\kappa a = 0.01$) is very different. In this case $-f_e$ and f_v decrease with increasing λ at small λ before increasing as $\lambda \to 1$. At small λ, the convective ion transport associated with the particle sedimentation decreases with increasing λ due to the additional drag on the fluid in the far boundary. This reduction in convective ion transport causes a corresponding reduction in Ψ_1 and C_{i1} and in turn $-f_e$. At higher λ, there is a sharp increase in the gradient in the equilibrium potential ($\nabla\Psi_0$), which corresponds to an increase in the equilibrium surface charge density of the sphere (at constant ζ_a). This causes a significant increase in the magnitude of the electri-

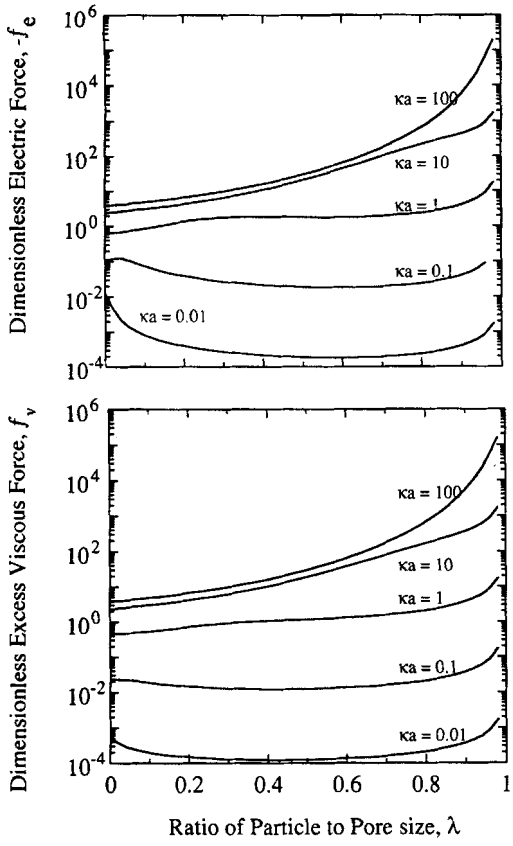

Figure 3. Dimensionless electric (top panel) and excess viscous (bottom panel) forces as a function of λ.

cal force on the particle. The variation of Ψ_1 and $\nabla\Psi_0$ with λ also determines the magnitude of the electrical forces acting on the fluid (electrolyte), leading to the observed dependence of the viscous force on λ at small κa. The situation is more complicated at intermediate κa. $\nabla\Psi_0$ increases monotonically with increasing λ, but Ψ_1 (and its derivative) go through a maximum at an intermediate value of λ due to the competing effects of the boundary on the flow. In this case the velocity gradient at the particle surface increases with increasing λ, causing an increase in $\nabla\Psi_1$, while the recirculation velocity at the outer boundary causes a decrease in $\nabla\Psi_1$ at larger values of λ. This causes a slight maximum in $-f_e$ followed by a weak minimum (similar to that seen at very small κa).

The total excess force ($f = f_e + f_v$) acting on the charged sphere is shown in Figure 4 as a function of κa at several values of λ. The results have been presented as $-f$, that is, the excess force always acts in the opposite direction of the gravitational field, reducing the sedimentation velocity compared to that for an uncharged particle. The results for $\lambda = 0$ are identical to those presented by Oshima et al. (1984) for the sedimentation of a charged sphere in an infinite medium. At small κa, the total excess force is dominated by f_e, which is proportional to κa for $\lambda = 0$ and to $(\kappa a)^2$ for the other λ. The behavior at very small λ is more complex, similar to that seen in Figure 2. The excess force at small κa decreases with increasing λ due to the reduction in the magnitude of Ψ_1 and C_{i1} arising from the increased drag on the fluid due to

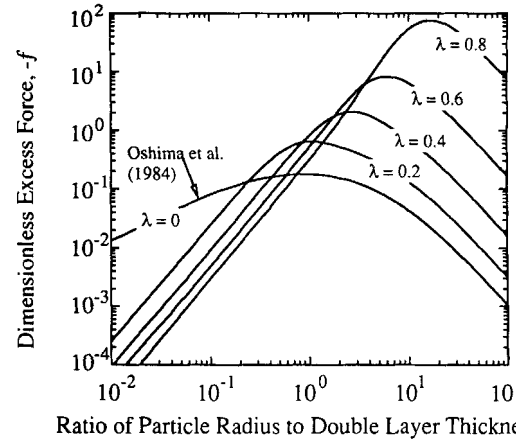

Figure 4. Total dimensionless excess force as a function of κa.

the pore boundary. The exact opposite behavior is seen at large κa, with $-f$ increasing by almost four orders of magnitude as λ goes from 0 to 0.08 at $\kappa a = 100$. This large increase in $-f$ is due to the large increase in the velocity gradient near the particle surface. As discussed previously, the leading order terms in f_v and f_e are equal in magnitude at large κa, but act in opposite directions. The first nonzero contribution to the total excess force at large κa is actually proportional to $(\kappa a)^{-2}$:

$$f = -\frac{12}{(\kappa a)^2}\,\frac{(1+2\lambda^3)}{(1-\lambda^3)}\,\frac{(2-5\lambda^3+3\lambda^5)^2}{(4-9\lambda+10\lambda^3-9\lambda^5+4\lambda^6)}, \quad (62)$$

which displays a very strong dependence on λ (Figure 4). Equation 62 reduces to $f = -12/(\kappa a)^2$ for the sedimentation of a charged sphere with an infinitely thin double layer in an unbounded medium, which is identical to the classic result developed by Smoluchowski (1921).

The maximum in the dimensionless excess force at intermediate κa reflects the transition from the behavior at small κa (where the double layer spans the pore) to the behavior at large κa (where the double layer is very thin). The results in Figure 4 for $\lambda \neq 0$ are well correlated as

$$(\kappa a)_{\max} = \frac{4\lambda}{1-\lambda}, \quad (63)$$

which is the point where the double layer thickness (κ^{-1}) is equal to one-quarter of the particle–pore separation ($b-a$). This maximum in f is related to the maximum in $\nabla\Psi_1$ discussed earlier.

General behavior at large κa

All of the results presented in the last section were for a spherical particle in a spherical cavity. It is also possible to develop a general expression for the total excess force on an arbitrary particle in the $\kappa a \to \infty$ limit using the basic procedure outlined earlier in this article. At large κa, the equilibrium electrical potential can be approximated as

$$\Psi_0 = \exp(-\kappa a z), \quad (64)$$

where z is the distance (in the direction of local normal) measured outward from the particle surface. Equation 64 is valid as long as the local surface curvature is much less than κ.

The electrical force on the particle is again given by Eq. 37, but in this case the surface integral can be converted to a volume integral since the contribution from any surface (boundary) sufficiently far from the particle (i.e., outside the electrical double layer) is identically equal to zero. The resulting volume integral for f_e (given by Eq. 52) is added to the expression for f_v (Eq. 42), with the total force given by Eq. 56. The only contribution to the required volume integral at large κa comes from the region very close to the particle surface. The volume differential (dV) is thus rewritten as $dz\,dS$ where dS is a differential area of the particle surface. Equation 56 can thus be written as

$$f = -\frac{(\kappa a)^2}{\pi}\int_S\int_z s u_z \frac{d\Psi_0}{dz}\,dz\,dS, \tag{65}$$

where u_z is the velocity component in the direction normal to the particle surface: $u_z = \boldsymbol{n}\cdot\boldsymbol{u}_0$. The first nonzero term in the Taylor series expansion for u_z is proportional to u_z'' since both u_z and $\partial u_z/\partial z$ are zero at the particle surface (the particle is impermeable and there is no normal stress at the particle surface). Equation 65 can thus be approximated as

$$f \approx -\frac{(\kappa a)^2}{\pi}\left[\frac{1}{2}\int_0^\infty z^2\frac{d\Psi_0}{dz}\,dz\right]\left[\int_S s(0,S)u_z''(0,S)\,dS\right], \tag{66}$$

where s has been evaluated at the particle surface ($z = 0$). Note that s and u_z'' are complex functions of the surface coordinate (S) with the detailed dependence determined by the specific geometry of the system. The value of s along the particle surface can be evaluated from Eqs. 43 and 44 using the method of Green's functions (Jackson, 1975):

$$s(0,S) \approx \langle s\rangle_S - 2\left[\frac{1}{2}\int_0^\infty z'^2\frac{d\Psi_0}{dz'}\,dz'\right] \times\left[\int_{S'} G(0,0,S,S')u_z''(0,S')\,dS'\right], \tag{67}$$

where $\langle s\rangle_S$ is the average value of s over the particle surface. The Green's function, G, corresponding to the Neumann problem defined by Eqs. 43 and 44, is again evaluated at the particle surface. The integration over z is performed with Ψ_0 given by Eq. 64, yielding

$$f \approx \frac{2}{\pi(\kappa a)^2}\int_S u_z''(0,S)\left[\int_{S'} G(0,0,S,S')u_z''(0,S')\,dS'\right]dS. \tag{68}$$

Note that the term involving $\langle s\rangle_S$ provides no contribution to the force because $\int_V \boldsymbol{u}_0\cdot\nabla\Psi_0\,dV$ is zero. Equation 68 provides a general expression for the dimensionless excess force on an arbitrary charged particle sedimenting in an arbitrary fluid (either unbounded or bounded) at large κa. Actual values for f can be determined by numerical integration if the velocity profiles for the uncharged particle [in particular $u_z(0,S)$] and the appropriate Green's function can be determined. Since both u_z and G are independent of κa, Eq. 68 clearly demonstrates that the dimensionless excess force at large κa is always proportional to $(\kappa a)^{-2}$, irrespective of the particle geometry or the bounded/unbounded nature of the system.

Hindered sedimentation and diffusion

The effects of the particle charge on the sedimentation velocity can be evaluated from Eq. 33 by setting $\boldsymbol{F}^*_{\text{total}}$ equal to zero. Calculations are shown in Figure 5 for a spherical particle in a spherical cavity for $q = 1$, $\zeta_a = 1$, $\zeta_b = 0$, and $\beta = 0.259$, the latter being characteristic of a KCl solution (van de Ven, 1993). The results have been normalized by the sedimentation velocity of the uncharged sphere:

$$\boldsymbol{U}_0 = \frac{\boldsymbol{F}^*_g K_{D_0}}{6\pi\mu a}, \tag{69}$$

where

$$\boldsymbol{F}^*_g = \frac{4}{3}\pi a^3(\rho_p - \rho)\boldsymbol{g}^* \tag{70}$$

and

$$K_{D_0} = \frac{\left(1 - \frac{9}{4}\lambda + \frac{5}{2}\lambda^3 - \frac{9}{4}\lambda^5 + \lambda^6\right)}{(1-\lambda^5)}, \tag{71}$$

where K_{D_0} is the hindrance factor for sedimentation of an uncharged sphere in a spherical cavity and is evaluated directly from the velocity and pressure profiles by setting $\boldsymbol{F}^*_{\text{uncharged}} = 0$ (Zydney, 1995). The presence of the surface charge reduces the magnitude of the sedimentation velocity,

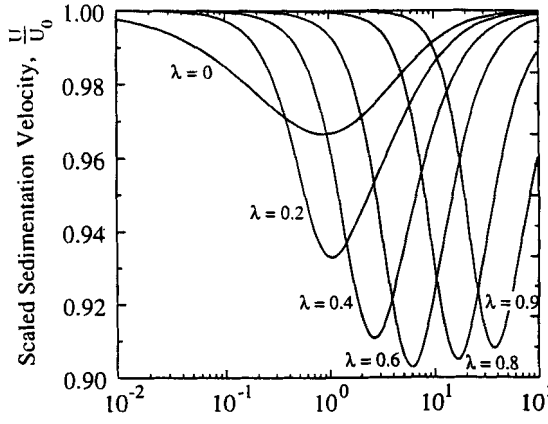

Figure 5. Scaled sedimentation velocity in an uncharged spherical cavity as a function of κa.

with the effect being greatest at an intermediate κa. The sedimentation velocity at very small κa is largely unaffected by the particle charge since the perturbation potential is quite small under these conditions. The sedimentation velocity at large κa is also only weakly influenced by the particle charge since the electrical force (f_e) exactly balances the excess viscous force (f_v) under these conditions. The location of the minimum in U/U_0 shifts to larger κa as λ increases, reflecting the shift in the transition from the small to large κa behavior discussed previously. The global minimum in U/U_0 occurs at $\lambda \approx 0.6$ and $\kappa a = 6$, even though the maximum in the excess force increases monotonically with increasing λ. This is due to the large reduction in K_{D_0} with increasing λ caused by the hydrodynamic interactions with the pore boundary. These interactions cause a large increase in $F^*_{\text{uncharged}}$, which more than compensates for the increase in the excess force.

The hindered diffusivity of a charged particle in a spherical cavity can be evaluated directly from the drag force using the Stokes–Einstein formalism (Deen, 1987). The results are conveniently expressed in terms of the enhanced drag coefficient, K_D, which is equal to the ratio of the drag force on the particle in an unbounded medium to the drag in the actual bounded geometry:

$$K_D = \frac{F^*_{\text{total}}(\lambda = 0)}{F^*_{\text{total}}(\lambda)}. \tag{72}$$

The hindrance factor can be evaluated directly from Eqs. 33, 36, and 41, yielding

$$K_D = K_{D_0}\left[\frac{1+\frac{\beta}{2}\left(1+\frac{1}{q}\right)\frac{\zeta a^2}{12}f(\lambda=0)}{1+\frac{\beta}{2}\left(1+\frac{1}{q}\right)\frac{\zeta_a^2}{12}f(\lambda)K_{D_0}}\right], \tag{73}$$

with K_{D_0} given by Eq. 71.

The effects of particle surface potential (ζ_a) and the electrolyte concentration (κa) on the hindrance factor for diffusion are shown explicitly in Figure 6 for $\lambda = 0.6$ using the same conditions examined in Figure 5 ($q = 1$, $\zeta_b = 0$, and $\beta = 0.259$). K_D displays a minimum at $\kappa a \approx 6$, with this effect becoming much more pronounced at higher values of the particle surface potential. This behavior is due to the greater effect of electrical interactions on the drag force (F^*_{total}) in the bounded system than that in the unbounded system. K_D actually increases with increasing surface potential at small values of κa due to the increase in F^*_{total} with increasing surface potential in the unbounded system. At these small values of κa, the electrical interactions in the bounded system are smaller than those in the unbounded system due to alteration of the potential fields caused by the pore boundary. The hindrance factor for the charged particle thus has a very complex dependence on κa, λ, and ζ_a.

Conclusions

Although the sedimentation velocity of a charged sphere at arbitrary double layer thickness was calculated many years ago by Booth (1954), there have been no corresponding investigations of the sedimentation of charged spheres in bounded systems despite the importance of electrical interactions on particle motion in a variety of porous media. This article describes a general procedure to evaluate the sedimentation velocity of a charged particle using a perturbation expansion in the particle surface potential and Peclet number. The excess viscous force is evaluated by application of the generalized reciprocal theorem developed by Tuebner (1982), thereby eliminating the need to determine the actual velocity and pressure field for the charged particle. This greatly simplifies the analysis, with the final expressions reducing to those developed previously by Booth (1954) and Oshima et al. (1984) for an isolated sphere sedimenting in an infinite medium.

Detailed calculations were performed for the boundary effects on the sedimentation of a charged sphere located at the center of a spherical cavity. At large κa, the forces exerted on the sphere increase sharply with increasing λ due to the effect of the pore boundary on the fluid velocity profiles near the particle (i.e., within the electrical double layer). The behavior at small κa is much more complex. Significant differences were seen in the behavior for the bounded and unbounded problems, with the dimensionless excess force being proportional to $(\kappa a)^2$ and κa in these two systems, respectively. This behavior was due to the effects of the boundary on both the equilibrium and perturbation potentials, the latter being influenced by the development of a recirculation flow in the bounded problem.

The analysis presented in this manuscript provides a generally applicable framework for the evaluation of the sedimentation velocity for charged particles. The behavior of an arbitrary particle in both an unbounded and bounded system at large κa was examined explicitly using the method of Green's functions. The dimensionless excess force under these conditions was shown to be proportional to $(\kappa a)^{-2}$ irrespective of the details of the particle and the pore geometry.

The complex dependence of the hindrance factor for diffusion on λ, κa, and the particle surface potential can have important implications for the transport of charged colloidal particles (e.g., proteins) through semipermeable membranes and chromatographic materials. In particular, the presence of the surface charge causes an even greater reduction in the particle diffusivity within the porous material than would have been predicted by partitioning alone. This behavior has in fact been observed experimentally by Pujar and Zydney (1994) in their study of albumin transport through a semipermeable polyethersulfone membrane. Pujar and Zydney showed that K_D is smallest (i.e., the hydrodynamic drag is greatest) at $\kappa a = 1.3$, which is in excellent agreement with the results shown in Figure 6. However, the magnitude of the variation in K_D with κa seen by Pujar and Zydney was considerably larger than that predicted in Figure 6. The reason for this discrepancy is uncertain. It may be due to the experimental difficulties involved in evaluating K_D from the membrane sieving experiments, the presence of a pore-size distribution in the membrane, and/or the complex charge distribution and regulation of the protein surface. The theoretical analysis developed in this manuscript provides the first theoretical explanation for these important experimental observations as well as an appropriate framework for evaluating the importance of boundary interactions on the sedimentation and hindered

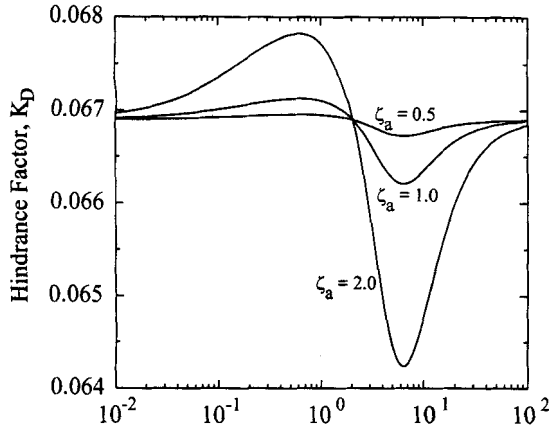

Figure 6. Hindrance factor for diffusion in an uncharged spherical cavity as a function of κa and ζ_a.

diffusion of charged particles in a wide vareity of porous media and membranes.

Acknowledgment

Narahari S. Pujar would like to acknowledge Philip K. Jackson at the University of Delaware for helpful discussions.

Notation

C_i = dimensionless concentration of ion i
C_{i0} = dimensionless equilibrium concentration of ion i
c_{i1} = dimensionless first-order perturbation to the concentration of ion i
E = electric field
F^*_{excess} = total excess force
F_{excess} = total dimensionless excess force
F^*_g = gravitational force
g = dimensionless gravitational acceleration
N_i = total dimensionless flux of ion i
P = dimensionless pressure
P_0 = dimensionless equilibrium pressure
p_0 = dimensionless pressure in an uncharged system
p_1 = dimensionless first-order perturbation in pressure
$S_{particle}$ = particle surface
S_{pore} = pore surface
t = time
U_0 = sedimentation velocity of uncharged sphere
v = dimensionless fluid velocity with the particle kept stationary
V^* = volume bounded by S_{pore} and $S_{particle}$
v_0 = dimensionless fluid velocity with the particle kept stationary
z = normal co-ordinate
β = dimensionless electrical force constant
ρ_p = particle density
ω = perturbation in ion concentration ($\omega = c_{+1} - c_{-1}$)
Ψ = dimensionless total electrical potential

Literature Cited

Bike, S. G., and D. C. Prieve, "Electrohydrodynamic Lubrication with Thin Double Layers," *J. Colloid Interf. Sci.*, **136**, 95 (1990).
Booth, F., "Sedimentation Potential and Velocity of Solid Spherical Particles," *J. Chem. Phys.*, **22**, 1956 (1954).
Deen, W. M., "Hindered Transport of Large Molecules in Liquid-Filled Pores," *AIChE J.*, **27**, 952 (1987).
Giddings, J. C., E. Kucera, C. P. Russell, and M. N. Myers, "Statistical Theory for the Equilibrium Distribution of Rigid Molecules in Inert Porous Networks. Exclusion Chromatography," *J. Phys. Chem.*, **72**, 4397 (1968).
Glandt, E. D., "Density Distribution of Hard Spherical Molecules inside Small Pores of Various Shapes," *J. Colloid Interf. Sci.*, **77**, 512 (1980).
Glandt, E. D., "Distribution Equilibrium between a Bulk Phase and Small Pores," *AIChE J.*, **27**, 51 (1981).
Haberman, W. L., and R. M. Sayre, "Motion of Rigid and Fluid Spheres in Stationary and Moving Liquids Inside Cylindrical Tubes," David W. Taylor Model Basin Rep. No. 1143, U. S. Dept. Navy, Washington, DC (1958).
Happel, J., and H. Brenner, *Low Reynolds Number Hydrodynamics*, Noordhoff, Leiden (1973).
Jackson, J. D., *Classical Electrodynamics*, Wiley, New York (1975).
Keh, H. J., and J. L. Anderson, "Boundary Effects on Electrophoretic Motion of Colloidal Spheres," *J. Fluid Mech.*, **153**, 417 (1985).
Kim, S., and S. J. Karrila, *Microhydrodynamics: Principles and Selected Applications*, Butterworth-Heinemann, Boston (1991).
Levine, S., G. Neale, and N. Epstein, "The Dorn Effect in a Concentrated Suspension of Spherical Particles," *Emulsions, Lattices and Dispersions*, P. Becher and M. N. Yudenfreund, eds., Marcel Dekker, New York (1978).
Oshima, H., T. W. Healy, L. R. White, and R. W. O'Brien, "Sedimentation Velocity and Potential in a Dilute Suspension of Charged Spherical Colloidal Particles," *J. Chem. Soc. Faraday Trans.*, **80**, 1299 (1984).
Potschka, M., "Size-Exclusion Chromatography of Polyelectrolytes: Experimental Evidence for a General Mechanism," *J. Chromatog.*, **441**, 239 (1988).
Pujar, N. S., and A. L. Zydney, "Electrostatic and Electrokinetic Interactions During Protein Transport through Narrow Pore Membranes," *Ind. Eng. Chem. Fundam.*, **33**, 2473 (1994).
Smoluchowski, M., *Handbuch der Elektrizitat und des Magnetismus*, Vol. II, L. Graetz, ed., Barth, Leipzig (1921).
Thies-Weesie, D. M. E., A. P. Philipse, G. Nagele, B. Mandl, and R. Klein, "Nonanalytical Concentration Dependence of Sedimentation of Charged Silica Spheres in an Organic Solvent: Experiments and Calculations," *J. Colloid Interf. Sci.*, **176**, 43 (1995).
Tuebner, M., "The Motion of Charged Colloidal Particles in Electric Fields," *J. Chem. Phys.*, **76**, 5564 (1982).
van de Ven, T. G. M., *Colloidal Hydrodynamics*, Academic Press, San Diego (1989).
van de Ven, T. G. M., P. Warzynski, and S. S. Dukhin, "Electrokinetic Lift of Small Particles," *J. Colloid Interf. Sci.*, **157**, 328 (1993).
Zydney, A. L., "Boundary Effects on the Electrophoretic Motion of a Charged Particle in a Spherical Cavity," *J. Colloid Interf. Sci.*, **169**, 476 (1995).

Manuscript received Aug. 22, 1995, and revision received Dec. 18, 1995.